SF2A 2014
J. Ballet, F. Bournaud, F. Martins, R. Monier and C. Reylé (eds)

SIMULATION OF THE MICROWAVE EMISSION FROM EXTENSIVE AIR SHOWERS

Sandra Le Coz[1]

Abstract. Ultra-high energy cosmic rays are detected through the extensive air showers they create when entering the atmosphere. The electromagnetic content of air showers is at the origin of different types of electromagnetic wave emissions, in different wavelength ranges. Air shower fluorescence light is detected routinely in ground-base detectors such as the Pierre Auger Observatory or Telescope Array. Decametric emissions (MHz) have been observed by different cosmic ray experiments equipped with antennas. Novel detection techniques based on the postulated GHz emission from molecular bremsstrahlung in air showers are also currently being studied. They are motivated by the observation of a microwave emission due to the low energy shower electrons generated by a high-energy electron beam passing through targets, in accelerator experiments. A fast simulation of this microwave emission from extensive air showers is reported here.

Keywords: cosmic rays, astroparticles, composition, radio, molecular bremsstrahlung

1 Introduction

1.1 Ultra-high energy cosmic rays

Cosmic rays are particles in relativistic motion through the interstellar and intergalactic media. They were discovered a century ago, through the particle showers they generate when entering the atmosphere. The detection of these shower particles was at the origin of the discovery of numerous subatomic particles, before the accelerator era. The increasing number of experiments dedicated to the detection of cosmic rays, at the ground, with balloons or in orbit, has allowed the measurement of the energy spectrum at Earth. Regardless of the energy, cosmic rays are mainly composed of protons and helium nuclei, including a fraction of heavier nuclei and electrons. At the highest energies, the flux is very low, reaching 1 particle per km^2 per year above 10^{19} eV. The question of the origin, the acceleration mechanisms and the mass composition of these ultra-high energy cosmic rays remains. Giant ground-based detectors are dedicated to their study. These detectors sample the particles of the air shower that reach the ground with a duty cycle of nearly 100% and/or detect the fluorescence light emitted along the air shower development, only on clear and moonless nights, that is about 10% of the time.

1.2 Fluorescence detection of extensive air showers

The fluorescence detectors of air shower experiments such as the Pierre Auger Observatory (The Pierre Auger collab. 2004, 2010) or Telescope Array (Tokuno & the Telescope Array collab. 2012) observe the shower's longitudinal development, collecting the fluorescence light emitted in the UV range by air-nitrogen, excited by the electrons of the shower. As the amount of collected light is related to the total deposited energy of the shower, fluorescence detectors allow the absolute energy calibration of surface detectors. Hence, the energy of cosmic rays may be inferred 100% of the time, on a model-free basis. As a proton interacts less with the atmosphere and generates a shower deeper than heavy nuclei (for the same total energy), the atmospheric depth X_{max} where the longitudinal development of the shower reaches the maximum number of particles is used to infer the mass. Because of shower to shower fluctuations and because of the overlap of proton and iron X_{max} distributions (the two extreme masses), the inference of mass is only possible stastistically and not event by event. Comparing the mean value and standard deviation of X_{max} with the values predicted by extrapolated

[1] Laboratoire de Physique Subatomique et de Cosmologie, Université Grenoble-Alpes, CNRS/IN2P3, Grenoble, France

hadronic models for proton and iron, the mass composition studied with Auger data is found to be compatible with protons up to 2×10^{19} eV and grows heavier as energy increases beyond this (The Pierre Auger collab. 2013). For Telescope Array, the mass composition is reported to be compatible with protons even at the highest energies (Tameda et al. 2013), but inference methods are a bit different. Due to the low flux and the low duty cycle of fluorescence detectors, the mass inference at the highest energies is statistically somewhat limited. A complementary detection technique may help to improve the situation : the radiodetection of air showers.

1.3 Radiodetection of extensive air showers

The electrons of air showers are not only related to fluorescence light, but are also at the origin of different types of electromagnetic wave emissions, in different wavelength ranges. Air shower decametric emissions (MHz) had been observed with aerials by different cosmic ray experiments (also using surface detector arrays) in the 50-60's, but the technique had sunk into oblivion in the 70's because of fluorescence detector developments. Triggered by the limitations of the latter, and by signal processing enhancements, a renewed interest has arisen in the 2000's. If fully realized, the radio detection (MHz or GHz) would offer a lot of advantages such as a low atmosphere attenuation and a near 100% duty cycle, to be compared to the 10% of fluorescence detectors. Recent experiments such as CODALEMA (in Nançay radio observatory; Ardouin 2005) and LOPES (using interferometry at Karlsrhue Institute of Technology; Falcke 2005) proved that the radio signal produced by an air shower allows to reconstruct its energy and direction. There is a consensus on the mechanisms at the origin of the emission: a geomagnetic deviation effect was identified in the 60's and a negative charge excess variation effect was confirmed around 2010 by the afore-mentioned experiments and by AERA (at the Pierre Auger Observatory; Schröder & the Pierre Auger collab. 2013; The Pierre Auger collab. 2014). All these MHz radiations are emitted anisotropically, along the shower axis.

Novel detection techniques based on the GHz emission from air showers are also being studied nowadays. They are mainly motivated by the observation by Gorham (2008) of a microwave emission thought to be due to low-energy electrons generated by a high-energy electron beam passing through targets, in an accelerator experiment at SLAC (Stanford). According to this purported mechanism of production, the GHz radiation may present the advantage of being emitted isotropically, and therefore to be detectable far away from the shower axis. Consequently, the Pierre Auger collaboration has been developing microwave (GHz) detection prototypes (Bérat & the Pierre Auger collab. 2013), such as AMBER (Gorham 2008), MIDAS (Alvarez-Muniz 2013), or EASIER (Gaior & the Pierre Auger collab. 2013), aiming to obtain valuable observables related to air showers.

2 Simulation of the GHz emission

2.1 Derivation of a molecular bremsstrahlung yield

The Gorham (2008) SLAC experiment consists of a beam of electrons passing through alumina targets, in order to create an electromagnetic shower that reaches a maximum of development when entering an anechoic chamber. In the chamber, antennas detect the radiation emitted at microwave frequencies by the shower. The recorded signal allows us to derive a yield for the microwave emission. We define this yield as the ratio between the energy deposited through microwave radiation per unit frequency, $E_{MW}/\Delta\nu$, and the total energy deposited, E_{dep}. Considering the features of the beam (and making an assumption on the number of electrons at the maximum of development), the features of the detection system, and the recorded signal, we get

$$Y_{MW} = \frac{E_{MW}/\Delta\nu}{E_{dep}} \sim 2 \times 10^{-18}\mathrm{Hz}^{-1}. \tag{2.1}$$

The radiation detected at SLAC has been understood as molecular bremsstrahlung radiation. Indeed, air shower electrons lose the main part of their energy by exciting or ionizing the air components : the oxygen and nitrogen. Nitrogen excitation is at the origin of the fluorescence light while air ionization is at the origin of secondary low-energy electrons. These secondary electrons interact in turn with the air, mainly with neutral components, more numerous than the ionized ones. This interaction between a low-energy electron and the electromagnetic field of neutral air molecules is quasi-elastic, and a bremsstrahlung radiation is emitted. As the secondary electrons are emitted without any favored direction, the bremsstrahlung radiation would be statistically isotropically emitted, and unpolarized. We derive now a phenomenological yield for the molecular bremsstrahlung emission.

The number of photons emitted per unit frequency per secondary electron depends on its velocity v, on the number of targets per unit volume n_m and on the interaction cross section Q,

$$\phi = n_m v Q. \tag{2.2}$$

According to Yamabe et al. (1983), the differential molecular bremsstrahlung (free-free interaction) cross section, per unit frequency ν of the emitted photon is given by

$$\frac{dQ}{d\nu}(e,\nu) = \frac{Q_{ff}}{\nu}(e,\nu), \tag{2.3}$$

where e is the kinetic energy of the electron and

$$Q_{ff}(e,\nu) = \frac{4}{3\pi}\frac{\alpha^3}{Ry} e \left(1 - \frac{h\nu}{2e}\right)\sqrt{1 - \frac{h\nu}{e}} Q_m(e), \tag{2.4}$$

with $\alpha = 7.3 \times 10^{-3}$ the fine-structure constant, $Ry = 13.6$ eV the Rydberg energy, $h = 6.63 \times 10^{-34}$ J.s the Planck constant, and $Q_m(e)$ the cross section for momentum transfer collisions of the electrons with the air targets. $Q_m(e)$ values are given for O_2 and N_2 in tables by Itikawa (2006, 2009). Considering only low frequency photons, we have $h\nu << e$. Equation 2.4 may therefore be rewritten as $Q_{ff}(e,\nu) = (4\alpha^3/3\pi Ry) e Q_m(e)$.

According to Opal (1971), the kinetic distribution of secondary electrons is expected to follow

$$f(e) = \frac{k}{1 + \left(\frac{e}{e_0}\right)^{2.1}}, \tag{2.5}$$

with $k \sim 1/20.9$ eV^{-1} the normalizing constant, $e_0(N_2) = 13$ eV and $e_0(O_2) = 17.4$ eV. This distribution is derived from experiments where primary electrons from 100 to 2000 eV scatter on oxygen and nitrogen.

The molecular bremsstrahlung radiation is limited by the attachment of electron to neutral dinitrogen, mainly occuring in 3 body reactions with 2 dinitrogen or with 1 dioxygen and 1 dinitrogen. According to Nijdam (2011), the lifetime of secondary electrons is expected to be

$$\tau = \frac{1}{n_m^2 (k_{att,1}[O_2]^2 + k_{att,2}[O_2][N_2])}, \tag{2.6}$$

depending on attachment constants $k_{att,1} = 2 \times 10^{-30}$ cm^6 s^{-1}, $k_{att,2} = 8 \times 10^{-32}$ cm^6 s^{-1}, on atmospheric components fractions $[O_2] = 0.2095$, $[N_2] = 0.7808$, and on the number of air molecules per unit volume, which has a value at sea level of $n_m = 2.58 \times 10^{19}$ cm^{-3}.

Knowing that the emitted power is equivalent to the number of photons emitted per unit time multiplied by the energy of photons $h\nu$, and taking into account the bremsstrahlung cross section, the energy distribution and the lifetime of secondary electrons, we get the total power emitted per unit frequency as a function of time by a set of $n_{e,0}$ secondary electrons,

$$\frac{P}{\Delta\nu} = n_{e,0} \exp\left(-\frac{t}{\tau}\right) \frac{4}{3\pi}\frac{\alpha^3}{Ry} n_m h \int_0^\infty v f(e) e Q_m(e) de. \tag{2.7}$$

To estimate the fraction of the energy deposited by the electrons of the shower through molecular bremsstrahlung, we define a yield

$$Y_{MBR} = \frac{E_{MBR}/\Delta\nu}{E_{dep}}, \tag{2.8}$$

with E_{MBR} the energy deposited by the electrons of the shower through molecular bremsstrahlung and E_{dep} the total energy deposited. Considering that E_{MBR} is the integral over time of the power derived above, and that to create the $n_{e,0}$ secondary electrons we need an energy $E_{dep} = n_{e,0} w_i$, with $w_i = 34$ eV the mean energy required to create an electron-ion pair in air (given by the ICRU Report 1993), we finally get

$$Y_{MBR}(z) = \frac{\tau}{w_i}\frac{4}{3\pi}\frac{\alpha^3}{Ry} n_m h \int_0^\infty v f(e) e Q_m(e) de \sim 6 \times 10^{-18} \frac{\rho_0}{\rho(z)} \text{Hz}^{-1}, \tag{2.9}$$

with $\rho(z)$ the density of the air regarding the altitude z and ρ_0 the density of the air at sea level. This phenomenological yield is of the same order of magnitude as the yield we derived from the results of the Gorham (2008) SLAC experiment at sea level.

2.2 Algorithm

To estimate the received signal at one antenna, we have to generate the air shower development, the molecular bremsstrahlung radiation, and to consider its propagation and the antenna response. In the simulation, the longitudinal development (number of electrons as a function of the atmospheric depth) of the air shower is given by the Gaisser & Hillas (1977) function, while the lateral extension of the shower is described by the NKG formula (Nishimura & Kamata 1958; Greisen 1960). Given the energy, the arrival direction and the mass of the cosmic ray, the shower is then generated. At each shower step, the energy emitted through bremsstrahlung is derived from the total deposited energy using

$$E_{MBR} = E_{dep} Y_{MBR} \Delta\nu, \tag{2.10}$$

with $\Delta\nu$ the antenna bandwidth. This energy is then split into pieces to take into account the secondary electrons lifetime. All the pieces of energy are then propagated to the antenna, taking into account the air index for radio waves, the distance between the emission step and the antenna, and the effective area of the antenna at the angle between its axis and the axis of propagation of the radiation to the antenna. The pieces of energy are then put into bins of time, according to their arrival time and to the digitization frequency of the antenna system. For each bin of time, the total energy is then divided by the duration of the bin and we finally get a signal in terms of power as a function of time, such as the signal depicted in Fig. 1.

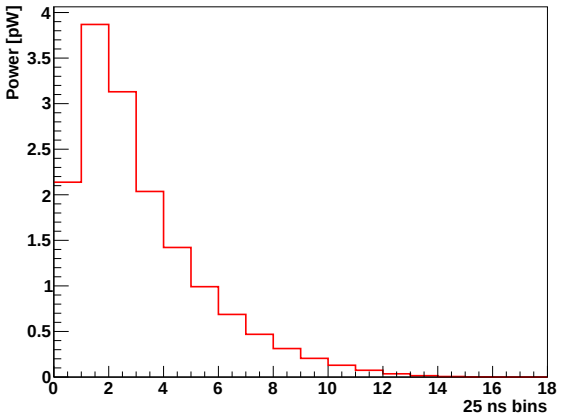

Fig. 1. Output of the simulation. Example of a simulated signal digitized at a frequency of 40 MHz.

2.3 Results

The simulation is carried out for a 10^{19} eV air shower. A proton is at the origin of the shower, with a zenith angle of 30°. The emitted radiation is detected at an altitude of 1400 m with a C-band LNBf (3.4-4.3 GHz), usually used for TV receiving, looking at the zenith. The signal is digitized at a frequency of 40 MHz. We consider two features of the signal, the maximum of the power and the number of 25 ns bins for which the power is above 10% of the maximum power. These features are depicted in Fig.2 as a function of the antenna position (X, Y coordinates) in the shower core frame. In this frame, the shower core is therefore in ($X = 0, Y = 0$), and the shower axis is along the positive part of the X-axis. After all, at 200 m from the shower core, we expect a maximum power of 6×10^{-12} W and 20 bins above 10% of the maximum power. At 1500 m, the maximum of the signal falls by 2 orders of magnitude and its duration is ten times longer.

3 Conclusions

The radiodetection of air showers would be attractive, in order to understand better the matter of the mass composition of ultra-high energy cosmic rays. We derived a bremsstrahlung yield, which has a value at sea level of $Y_{MBR}(z) \sim 6 \times 10^{18}$ Hz^{-1}, that is the same order of magnitude as the yield we derived from the Gorham (2008) SLAC experiment results. For a 10^{19} eV air shower, we simulated the signal detected by a C-band

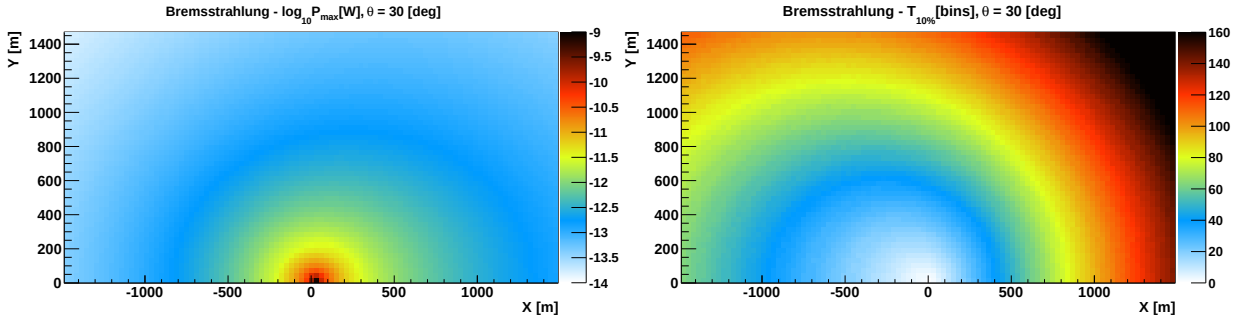

Fig. 2. Features of the simulated signal as a function of the antenna position in the shower-core frame (see text). **Left:** Logarithm of the maximum of the power in pW. **Right:** Number of 25 ns bins for which the power is above 10% of the maximum power.

TV-antenna. At a few hundred meters from the shower core, we estimated the signal to be of an order of magnitude of 1 pW, and to last a few tens of 25 ns bins.

I acknowledge the support of the Joseph Fourier University and of the French Agence Nationale de la Recherche 321 (ANR) under reference ANR-12-BS05-0005-01. I also thank the Pierre Auger collaboration and the SF2A local organization committee.

References

Alvarez-Muniz, J. *et al.*. 2013, Nucl. Inst. Meth. Phys. Res., 719, 70
Ardouin, D. *et al.*. 2005, Nucl. Instrum. Meth. A, 555, 148
Bérat, C. & the Pierre Auger collab. 2013, Nucl. Instr. and Meth. A, 718, 471
Falcke, H. *et al.*. 2005, Nature, 435, 313
Gaior, R. & the Pierre Auger collab. 2013, ICRC (Rio de Janeiro)
Gaisser, T. K. & Hillas, A. M. 1977, 15th ICRC, 8, 353
Gorham, P. W. *et al.*. 2008, Phys. Rev. D, 78, 032007
Greisen, K. 1960, Ann. Rev. Nucl. Part. Sci., 10, 63
ICRU Report. 1993, 31
Itikawa, Y. 2006, J. Phys. Chem, 35, 31
Itikawa, Y. 2009, J. Phys. Chem, 38, 1
Nijdam, A. 2011, ApJ, 44, 455201
Nishimura, J. & Kamata, K. 1958, Progr. Theor. Phys., 6, 93
Opal, C. B. 1971, J. Chem. Phys., 55, 4100
Schröder, F. G. & the Pierre Auger collab. 2013, ICRC (Rio de Janeiro)
Tameda, Y., the Telescope Array, & Hires collab. 2013, EPJ Web Conf., 53, 04005
The Pierre Auger collab. 2004, Nucl. Instrum. Meth. A, 523, 50
The Pierre Auger collab. 2010, Nucl. Instr. and Meth. A, 620, 227
The Pierre Auger collab. 2013, JCAP, 026, 02
The Pierre Auger collab. 2014, Phys. Rev. D, 89, 052002
Tokuno, H. & the Telescope Array collab. 2012, Nucl. Instr. and Meth. A, 676, 54
Yamabe, C., Buckman, S. J., & Phelps, A. V. 1983, Phys. Rev. A, 27, 3